

# Photometry and spectroscopy of SN 2015bh in the galaxy NGC 2770

V. P. Goranskij,<sup>1</sup> <sup>★</sup> E. A. Barsukova,<sup>2</sup> A. F. Valeev,<sup>2,3</sup> D. Yu. Tsvetkov,<sup>1</sup>

I. M. Volkov,<sup>1</sup> V. G. Metlov,<sup>1</sup> A. V. Zharova<sup>1</sup>

<sup>1</sup>*Sternberg Astronomical Institute, Lomonosov Moscow State University, Universitetsky Prospect, 13, Moscow 119899 Russia*

<sup>2</sup>*Special Astrophysical Observatory of the Russian Academy of Sciences, Nizhnij Arkhyz, Karachay-Cherkessia 369167 Russia*

<sup>3</sup>*Kazan Federal University, Kremlevskaya street 18, Kazan, Tatarstan 420008 Russia*

30 October 2018

## ABSTRACT

We present medium-resolution spectroscopy and multicolor photometry for the optical transient PSN J09093496+3307204 (SN 2015bh) in the galaxy NGC 2770, which has transferred into the supernova phase. The observations were carried out between February 2015 to May 2016. Both at the phase of the SN impostor (2015a) and at the supernova phase (2015b), besides Balmer emissions, the strong Fe II emissions are seen in the spectrum; so, these spectra resemble those of Williams Fe II type classical novae. The star is located near the edge of a dark nebula and notably absorbed ( $A_V = 1^m14 \pm 0^m15$ ). Taking into account this absorption, we determined maximum absolute magnitudes of  $M_V = -15^m0 \pm 0^m3$  at the 2015a phase and of  $M_V = -18^m14 \pm 0^m30$  at the 2015b phase. The light curve at the 2015b phase is similar to those of SN IIL. The supernova progenitor is a luminous blue variable (LBV) star with the powerful  $H_\alpha$  emission. We considered several hypotheses of supernovae explosions following optical transients related with LBV. The hypothesis of core collapse of an evolved massive star interrupting the process of its merging with massive companion in a binary system (a failed luminous red nova) was chosen as the preferable one for this event.

**Key words:** stars: supernovae, impostors, luminous red novae, supernovae, photometry, spectroscopy — stars: individual: SN 2015bh, PSN J09093496+3307204

<sup>★</sup> Contact e-mail: [goray@sai.msu.ru](mailto:goray@sai.msu.ru)

## 1 INTRODUCTION

The optical transient PSN J09093496+3307204 was discovered in the galaxy NGC 2770 on February 7, 2015 in the Catalina Real-Time Transient Survey, and on February 8, 2015 by S. Hoverton in the process of observations under the program SNhunt<sup>1</sup>. The transient is also known as SN 2015bh and SNhunt275. In the spectrum obtained in Asiago Observatory on February 9, a broad emission  $H_\alpha$  (FWHM  $\sim 6800 \text{ km s}^{-1}$ ) with a narrow line with P Cygni profile on top was visible (Elias-Rosa et al. 2015). The absorption component of the profile showed the expansion velocity  $\sim 950 \text{ km s}^{-1}$ . In 2008 – 2009 HST images, a faint star was detected coinciding in coordinates with the transient and variable within  $21^m.5 - 22^m.8$  in the red filter F606W. Its spectrum and chaotic variability resembled supernova impostors 2000ch and 2009ip, before the explosion of latter as a supernova in June 2012 (Elias-Rosa et al. 2015). The definition of "supernova impostor" was introduced by Van Dyk et al. (2000) to identify the explosions of LBV stars in which stars survived and being observed several years after outbursts in contrast to SN IIn, which were destroyed at the core collapse. The eruption of  $\eta$  Car in 1844 – 1850 can be an analog of a SN impostor. So, the transient in NGC 2770 was classified as a SN impostor or an LBV explosion.

Photometry and spectroscopy with the 10.4 m GTC telescope at Canarias within the time interval between March 27 and April 14, 2015 revealed a considerable increase of star brightness by  $1^m.2$ , and the object reached the absolute magnitude  $-14^m.2$  in the SDSS  $r$  band (de Ugarto Postigo et al. 2015a). In the spectrum taken on April 14, the  $H_\alpha$  emission, other Balmer lines, the distinct emissions Fe II in the range  $\lambda 4950-5400 \text{ \AA}$  and the Na I/He I blend were predominating. The  $H_\alpha$  line profile was asymmetric with a red-side wing extending up to  $\sim 5000 \text{ km s}^{-1}$ , and a steeper blue-side decline. But the P Cyg type profile in  $H_\alpha$  line was already not observable.

On May 16, 2016, de Ugarto Postigo et al. (2015b) informed about a sharp increase of the transient brightness by  $2^m$ . The absolute magnitude in the  $R$  band reached  $-16^m.4$ . In new spectra of May 16 from the Keck I telescope, the star displayed a hot continuum with Balmer, He II and He I emission lines (Duggan et al. 2015).  $H_\alpha$  remained asymmetric with the half-width FWHM  $\sim 1200 \text{ km s}^{-1}$ . It became clear that it was a new explosion of the impostor, and the events were developing according to the scenario of SN 2009ip (Mauerhan et al. 2013; Margutti et al. 2014; Graham et al. 2014; Pastorello et al. 2013). The observations continued by Campana et al. (2015); Vinko et al. (2015) and Richardson et al. (2015) confirmed the assumptions that the transient passed to the

<sup>1</sup> <http://www.rochesterastronomy.org/sn2015/snhunt275.html>

SN II phase. By analogy with other papers, we designate the first outburst or the impostor phase as 2015a and the second brightening or the SN phase as 2015b.

The host galaxy of SN 2015bh, NGC 2770 is located at a distance of  $d = 29.70 \pm 3.4$  (distance module  $M - m = 32^m35 \pm 0.24$ ); its radial velocity is  $v_r = 1947 \text{ km s}^{-1}$  (redshift  $z = 0.006494$ ); the Galaxy extinction in this direction is  $A_V = 0^m062$  (NED). Before the 2015 event, three SNe of the rare Ib type exploded in the galaxy NGC 2770 during a short period of 10 years, that is why the galaxy was called "a factory of type Ib supernovae" (Thöne et al. 2015). These are SNe 1999eh, 2007uy and 2008D. The latter one is interesting by the fact that it was related to an X-ray transient. Thöne et al. (2015) show in their Fig. 1 the galaxy image assembled from three VLT frames of March 16, 2008, including one with the filter centered on  $6604 \text{ \AA}$  at  $z = 0.007$  and the width  $64 \text{ \AA}$ , and another one in the filter  $H_\alpha$  at  $z = 0$  with the center at  $6563 \text{ \AA}$  and the width  $61 \text{ \AA}$ . Besides the two SNe of 2007 and 2008, one can see there a SN 2015bh progenitor, which is distinguished by its excess of emission in the  $H_\alpha$  line. This is one of the brightest stars of the galaxy.

## 2 PHOTOMETRY

Photometry in the Johnson *UBV* and Cousins *RI* bands was taken with the focal reducer SCORPIO at the BTA (Afanasiev & Moiseev 2005) in the process of spectral observations. Additionally, CCD photometers were used at the 1-m telescope of SAO RAS, at the 70-cm telescope of SAI MSU in Moscow, at the 60-cm reflector and the 50-cm Maksutov meniscus telescope of the Crimean Observational Station of MSU, and at the 1-m and 60-cm telescopes of the Simeiz Observatory in Crimea. Our observations were performed in the period from February 24, 2015 to May 30, 2016 with a break from June 16 to September 10, 2015, when the object was not observed due to conjunction with the Sun. The first images after the break suitable for measurement were obtained with the 1-m telescope of SAO RAS in the  $R_C$  and  $I_C$  filters on September 11, 2015, against the dawn background. The standard stars from Modjaz et al. (2009) near NGC 2770 in the Johnson *UBV* and Cousins *RI* system were used as comparison stars. Altogether we have 43 observations, both multicolor ones and those taken in individual filters. They are listed in Table 1. The full collection of observations of SN 2015bh including published observations of other au-

thors and supplemented by new data is available in Internet<sup>2,3</sup>. The light and color curves can be examined with a Java-compatible browser<sup>4,5</sup>.

The accuracy of measurements is given in Table 1 in brackets after each observation in units of the last significant digit. The Table comment contains information on telescopes and detectors used in observations. There are small systematic differences between sets of our observations obtained with different devices. These differences were determined from simultaneous measurements and compensated for corrections. After the conjunction with the Sun when the star brightness was faint, we were accumulating signal from the star during a long time, 1300 – 6000 s, to achieve a high signal-to-noise ratio. The main factor of the errors during long accumulation was an inhomogeneous surrounding background of the galaxy, because the star is located in a spiral arm near a dark dust nebula. Fig. 1 presents fragments of images with the highest angular resolution taken with the Hubble Space Telescope and with the ground-based telescope Gemini (a fragment of the color image by S. Rankin in Flickr.com). The progenitor, an LBV star is identified in the image. The HST images have been already analyzed by [Elias-Rosa et al. \(2015\)](#). We have measured the color image of Gemini of March 6, 2008 composed from components in the SDSS *gri* filters and  $H_\alpha$  filter by decomposing it into RGB components. The faintest stars from the SDSS database in the vicinity of the galaxy NGC 2770 were used as comparison stars. At that moment the star brightness was  $g = 25^m4 \pm 0^m15$  and  $r = 25^m0 \pm 0^m2$  in the system AB95. These values correspond to  $V = 25^m2$ . In the filters  $i + H_\alpha$  the star was much brighter,  $23^m3 \pm 0^m2$ .

The  $BVR_CI_C$  light curves are shown in Fig. 2 (from bottom to top). Besides our observations, here the data published by [Elias-Rosa et al. \(2015\)](#); [de Ugarto Postigo et al. \(2015a\)](#) (converted from SDSS values to the  $UBVR_CI_C$  system) and by [Campana et al. \(2015\)](#); [Vinko et al. \(2015\)](#) are collected. These observations and our ones are shown by points. Observations from a collection of S. Hoverton<sup>6</sup>, A. Cason and R. Arbour<sup>7</sup> are plotted on the  $V$  band light curve by circles. These observations were made with different CCDs and mainly without filters, but they are consistent with our observations in the  $V$  filter rather well. Triangles denote observations by Zhijian Xu and Xing Gao from the Hoverton's collection. The first observation (2015 April 7.74 UT, mag = 17.8, no filter) is considerably (by  $0^m8$ ) brighter than the mean light curve and the observation by

<sup>2</sup> <http://jet.sao.ru/~goray/psn0909.ne3>

<sup>3</sup> <http://vgoranskij.net/psn0909.ne3>

<sup>4</sup> <http://jet.sao.ru/~goray/psn0909.htm>

<sup>5</sup> <http://vgoranskij.net/psn0909.htm>

<sup>6</sup> <https://www.flickr.com/photos/watchingthesky/17162602585/>

<sup>7</sup> <http://www.rochesterastronomy.org/sn2015/snhunt275.html>

de Ugarto Postigo et al. (2015a) obtained at nearly the same time. It is possible that they registered a short flare. Separate observations by G. Locatelli (Flickr.com) and G. Masi (CBAT) are also plotted with circles.

The phase 2015a is covered by observations from December 21, 2014 to April 25, 2015, or within JD 2457013 – 2457138. At that time photometry shows a gradual rise of brightness with an average rate of  $0^m015$  per day ( $0^m75$  during 50 days). The observed brightness fluctuations in amplitude were of several tenths of a magnitude, there were a short brightness weakening by  $0^m9$  near JD 2457066 and brightness decline by about  $1^m$  before the rise to the main maximum. At the phase 2015a, the star achieved the level  $18^m4$  (CCD without filter). The decline of brightness before the rise to the main maximum (JD 2457153,  $19^m3$ ) registered by Hoverton is a very important observation for the understanding the nature of 2015bh, but it should be noted that this observation is single. The SN brightness rise (the beginning of the phase 2015b) has been registered starting from May 13, 2015 (JD 2457156). The brightness maximum of the phase 2015b was on May 22, 2015, at the moment JD  $2457165 \pm 1^d$ . Maximum magnitudes at the phase 2015b were as follows:  $U = 14^m75$ ,  $B = 15^m57$ ,  $V = 15^m35$ ,  $R_C = 15.21$ ,  $I_C = 15.10$  measured with the SAO 1 m telescope, and  $B = 15^m54$ ,  $V = 15^m35$ ,  $R_C = 15^m18$  measured with the 60 cm telescope of Simeiz Observatory. In the SN light curve (2015b), we allocate the initial linear decay of brightness after maximum of May 22 – October 17, 2015 (JD 2457165–2457313) and the secondary decay after October 17, 2015 (JD > 2457313). An abrupt transition in the brightness decay rate from the initial one to the secondary one is seen in all bands except  $I_C$ . In the initial decay in the first 50 days, the rates of brightness decline in the  $BVR_CI_C$  filters were, respectively,  $2^m0$ ,  $1^m5$ ,  $1^m3$  and  $1^m0$ . A sharp peak in the maximum and a linear brightness decay in the magnitude scale continued during  $\sim 150$  days after the maximum are typical for light curves of SN IIL. A considerable part of this period, the star was inaccessible for observation. However, September observations in the  $R_C$  and  $I_C$  filters carried out in SAO RAS right after appearance of the object from behind the Sun confirm the linear character of the initial decay. The mean light curve of SNe IIL<sup>8</sup> shows that the brightness decline rate changes within the range of  $2^m2 - 3^m0$  during 50 days in the  $B$  filter. SN 2015bh demonstrates a lower brightness decay rate ( $2^m0$ ) in comparison with this summary light curve. Yet, when comparing the decay rate in the  $V$  filter with three separate SNe IIL 1980K ( $1^m9$ ), 1998S ( $1^m5$ )<sup>9</sup> and 2008if ( $1^m4$ ) (Anderson et al. 2014) the light curve of SN 2015bh looks typical for SNe IIL. Then, in the secondary decay at the end of October 2015, the rate of brightness

<sup>8</sup> <http://burro.cwru.edu/academics/Astr221/LifeCycle/observingSN.html>

<sup>9</sup> <http://dau.itep.ru/sn/lc>

decline reduced considerably, especially in the filter  $R_C$ . The slowest brightness decay rate in  $R_C$  is obviously related to a gradual increase of contribution of the  $H_\alpha$  emission along with the weakening of continuum in the long-wave range. In Fig. 2, the heavy gray line shows the secondary light decay rate due to radioactive decay of the  $^{56}\text{Co}$  isotope (as in SNe I and in several SNe II). The average slope in the 200-day secondary brightness decay in the  $V$  filter (where the contribution of emission lines is minimum) was  $0^{\text{m}}0092$  per day ( $0^{\text{m}}46$  during 50 days), what corresponds to the hypothesis of the  $^{56}\text{Co}$  decay rate and confirms the assumption that the event 2015b was a SN.

The color-index  $B - V$ ,  $V - R_C$  and  $V - I_C$  curves are presented in Fig. 3 together with the  $V$  light curve in the scale of absolute  $V$  magnitudes (right). When plotting the color curves, we used not only simultaneous observations obtained in separate nights, but also the observations in consecutive nights in the interval 1–2 days. When the star was faint, and the light accumulation time amounted to 2 hours, it was impossible to do that for all filters during one night. On the other hand, in the secondary decay, the changes of the object brightness during 2 days were much lower than measurement errors, so, the color indices are quite realistic. At the phase 2015a,  $B - V$  and  $V - R_C$  color indices were gradually reducing, what reflected increasing star's temperature. However, the  $V - I_C$  trend was opposite. At the explosion of SN at the phase 2015b, the star was the hottest in the rising branch at the moment JD 2457159, i.e. 6 days before maximum, with the color indices  $U - B = -0^{\text{m}}85$ ,  $B - V = +0^{\text{m}}08$  (this is data of SWIFT/UVOT in the system  $ubv$  AB (Campana et al. 2015), converted into the Vega  $UBV$  system). This fact is confirmed by spectral observations with the Keck telescope (Duggan et al. 2015), when the hot continuum and the He II 4686 Å emission were observed. Taking into consideration the fact that at that time  $UBV$  bands were predominated by the hot continuum, and the contribution of emissions was small (it is expected to be <3%) we determined the color excess  $E(B - V) = 0^{\text{m}}37 \pm 0^{\text{m}}05$  and extinction  $A_V = 1^{\text{m}}14 \pm 0^{\text{m}}15$ . This estimate of interstellar extinction includes both the extinction in our Galaxy and that in the galaxy NGC 2770 together with the circumstellar environment. With due regard to such extinction along the line of sight, the absolute visual magnitude of SN in the brightness maximum was  $M_V = -18^{\text{m}}14 \pm 0^{\text{m}}30$ , and in the impostor stage it achieved  $M_V = -15^{\text{m}}0 \pm 0^{\text{m}}3$  (or even  $M_V = -15^{\text{m}}7$ , if relying on the observation by Zhijian Xu and Xing Gao discussed above). Thus, it follows from observations that the event 2015b with its light curve shape and absolute magnitude in maximum can be interpreted as a real SN.

From measurements of minimum brightness on March 6, 2008, with the telescope Gemini  $V = 25^{\text{m}}2 \pm 0^{\text{m}}3$  with allowance made for extinction, the absolute magnitude of the SN 2015bh progenitor was  $M_V = -8^{\text{m}}3 \pm 0^{\text{m}}3$ . This is close to the Humphreys & Davidson (1979) limit for



the most massive stars and confirms classification of the progenitor as an LBV. Stars of so high luminosity are not stable, they lose their mass and form the circumstellar medium rich with gas and dust.

Starting from the first moment of registration of the SN on the ascending branch of the 2015b outburst, a gradual reddening in all the color indices continued until the break in observations caused by conjunction with the Sun. It is obvious that this reddening occurred due to expansion of the ejected optically thick gas shell and decreasing of surface temperature of this shell. However, after the break in observations, the behavior of color indices changed.  $B - V$  and  $V - I_C$  indices became bluer and revealed opposite trends in their changes, whereas the reddening of  $V - R_C$  continued with the same rate. We explain that behavior by transition of the shell in the optically thin state, what leads to the fact that the radiation passes from hot inner layers of the shell. However, in the  $V - R_C$  index, the contribution of the  $H_\alpha$  emission increases relative to the hot continuum, and the increase of this index continues. The color index  $V - R_C$  increased by 1<sup>m</sup>.4 during 9 months after the brightness maximum. Similar changes of color indices occur in some classical novae, and they are related to analogous changes in the structure of ejected shells.

### 3 SPECTROSCOPY

Moderate-resolution spectral observations were carried out with the Russian 6 m telescope BTA and the focal reducer SCORPIO (Afanasiev & Moiseev 2005) during 8 nights in the period between February 23, 2015 and May 30, 2016. The observations were obtained 88 and 87 days before the SN brightness maximum, in the initial brightness decay 22 days after this maximum, and in the secondary decay, in the time range between 176 to 374 days after the maximum. Table 2 contains main information on the spectra: date, and Julian date, time in days counted from the brightness maximum, full exposure in seconds, spectral range, spectral resolution, grism, heliocentric corrections to radial velocities, and signal-to-noise ratio in continuum in the middle of the spectral range. Naturally, the signal-to-noise ratio in the profiles of spectral lines is much higher. The spectra were processed in OS Linux using the ESO MIDAS package and the LONG context (for the long-slit spectra). In the red wavelength range of  $\lambda > 6800 \text{ \AA}$ , the spectra are distorted by interference pattern (fringes). Since the signal-to-noise ratio in spectra obtained in November 2015 and later is too small (2–4), we smoothed them by the moving-average method with the averaging interval  $3.5 - 15 \text{ \AA}$ , which is equal to actual spectral resolution of each spectrum. To convert the spectra into energy units, we used spectrophotometric standards by Oke (1990) and simultaneous

photometric observations. The spectra are available in digital form in Internet<sup>10</sup>. The moments of our spectral observations are plotted in the light curve (Fig. 3, *Sp*). Spectral observations published by other authors are also marked in the Figure with (*ps*); these spectra or their descriptions are available in Internet.

Fig. 4 shows the spectra of SN 2015bh in the blue and green range at the phase 2015a (top) and at the phase 2015b immediately after the brightness maximum (bottom). The total spectrum of the star at the phase 2015a composed of the spectra taken on February 23 and 24, 2015 including the red range is shown in Fig. 5 (top). Approximately, these spectra correspond to descriptions given by Elias-Rosa et al. (2015); de Ugarto Postigo et al. (2015a) and de Ugarto Postigo et al. (2015b).

In the spectrum of February 23, 2015 at the phase 2015a, the  $H_\alpha$  profile consists of a narrow emission line with a weak absorption component shifted to the blue side, both ones superimposed on a broad emission base. The emission peak is at a velocity of  $1900 \text{ km s}^{-1}$ , or, taking into account the galaxy redshift, at  $-47 \text{ km s}^{-1}$ . The width of the narrow emission component at the half-maximum intensity level corrected for the instrument profile, *FWHM* is  $640 \text{ km s}^{-1}$ . This component has an emission hump in the red wing at a velocity of  $+870 \text{ km s}^{-1}$ . The narrow absorption component is located at a velocity of  $-900 \text{ km s}^{-1}$ , symmetrically relative to the emission maximum. These velocities are measured relative to the emission peak. The wide wings of  $H_\alpha$  emission extend up to  $10000 \text{ km s}^{-1}$  to each side from the peak. The  $H_\beta$  line profile has the identical structure, there is also a hump at a velocity of  $+870 \text{ km s}^{-1}$ . In emission of this line, one can trace only the short-wavelength wing extending up to  $-8500 \text{ km s}^{-1}$ . The long-wavelength wing is distorted by strong Fe II emission lines. Undoubtedly, the wide wings of Balmer lines are not related to motions of large mass of material, but they result from Thomson scattering of Balmer photons by free electrons. The strongest Fe II lines show the P Cyg type profiles.

In the blue spectrum of June 13, 2015 (the phase 2015b), a wide and deep absorption component extending to the velocities  $-4000 \text{ km s}^{-1}$  appeared in the profiles of Balmer lines. In the depth of this component, a narrow absorption detail at a velocity  $-900 \text{ km s}^{-1}$  observed previously at the phase 2015a, remained, and a new absorption detail at a velocity of  $-1900 \text{ km s}^{-1}$  appeared (these details were marked in Fig. 4). Similar absorptions with double absorption details were observed in the strong Fe II lines at the phase 2015b. A considerable asymmetry of emission components in the P Cyg profiles of  $H_\alpha$ ,  $H_\beta$ , strong emissions Fe II, their triangle shape are due to excess absorption in the blue wing of the profile within the velocity range between  $-3300$  and  $-250 \text{ km s}^{-1}$ .

<sup>10</sup> <http://jet.sao.ru/~bars/spectra/psn0909/>



(This fact can be set if superimpose the profile with its mirror reflection, as was done, e.g., in Fig. 6 by [Smith et al. \(2016\)](#) for the spectrum of the luminous red nova NGC 4490-OT2011). Such a structure of profiles is formed by dense optically-thick ejected shell, its formation continued as early as at the phase 2015a. The observation of hot continuum with the Balmer emissions, the lines He II and He I on May 16, 2015 by [Duggan et al. \(2015\)](#) indicated the exit of shock wave at the brightness rise of the 2015b outburst. Because of this, during a month, the high-velocity absorption components appeared in the profiles, but the component with a velocity of  $-900 \text{ km s}^{-1}$  formed before the 2015 events, remained in the line profiles. It is formed in a medium where the shock wave has not reached yet. At the phase 2015b a part of this medium got acceleration by the light pressure of the outburst, and the second narrow absorption component at a velocity of  $-1900 \text{ km s}^{-1}$  arose. The interesting observational fact is that the velocity of the narrow absorption component  $-900 \text{ km s}^{-1}$  in the blue wing of the Balmer line profiles is equal but oppositely directed to the velocity of the emission component (hump) in the red wing. This may mean that the initial medium was formed by a bipolar wind which was outflowing at a big space angle. A part of this conic outflow directed to the observer absorbs the light of the optically thick shell, and the opposite part is seen in emission. Besides, these narrow components show that the primary circumstellar medium was expanding to considerably larger distances than photosphere of the ejected shell forming the P Cyg type profiles.

Strong Fe II lines are a typical feature of the SN 2015bh spectra at both phases, 2015a and 2015b. With these lines, the spectra resemble ones of [Williams \(2012\)](#) Fe II type classical novae more, than those of supernovae. Classical novae are cataclysmic or symbiotic systems comprising a far-evolved star (a white dwarf) and a normal companion (a red dwarf or a red giant) which is an accretion donor. The outburst of a nova is a thermonuclear runaway of a hydrogen envelope accumulated on the surface of a white dwarf due to accretion. Of course, the SN 2015bh explosion scale exceeds the scale of classical novae. Its luminosity at the phase 2015a exceeds the maximum luminosity of brightest classical novae 100 times, and at the phase 2015b does 1600 times. The formal resemblance between spectra of novae and SN 2015bh demands a detailed study, because [de Ugarto Postigo et al. \(2015a\)](#); [Duggan et al. \(2015\)](#) note presence of the He I and even He II lines, which are not observed in Fe II type classical novae except rare cases of hybrid novae. Classical novae of another type, the Williams He/N, have the He I and He II lines, and this is the main sign of the He/N type, but the iron lines are not found in their spectra. The strongest He I lines in the optical spectrum are expected at the wavelengths 4121, 4143, 4388, 4471, 4713, 4922, 5016, 5876 and  $6678 \text{ \AA}$ . Resolution of our spectra is sufficient to determine that the He I

components are absent in possible blends with strong emissions of Fe II 4922 and 5018 Å (the multiplet 42), and in the blend with Na I 5889/5896 Å at the phase 2015b. The emission peaks at 4922 and 5018 Å coincide with other Fe II lines in radial velocity. Other He I lines were also not detected. There is a faint detail in the region of He I 4471 Å in the spectrum of June 13, 2015 on the 22 day after the maximum at the 2015b phase, the identification of which with the helium line is doubtful. Other He I lines including components of the Fe II blends mentioned above are not detectable. Besides two mentioned in our spectra, Fe II emissions are reliably identified at the following wavelengths in Angstroms (the multiplet number is in brackets): 4179(28), 4233(27), 4303(27), 4352(27), 4417(27), 4523(38), 4556(37), 5169(42), 5198(49), 5235(49), the blend 5276(49)+5284(41), 5317(48,49), 5363(48) and 5425 (48,49). All these lines are available in the list of emission lines of classical novae in optical range (Table 2, [Williams \(2012\)](#)). Besides these lines, we have found two lines at 4590 and 4635 Å which are absent in this list. Both emissions are strong in our spectra of the Williams Fe II type classical nova V496 Sct obtained on November 10 and 11, 2009. According to Fig. 1.10 by [Humphreys & Martin \(2012\)](#), both lines are available in the  $\eta$  Car spectrum where they are identified as the blends Fe II and Cr II. At the phase 2015a, the absorption component of strongest lines Fe II 4924, 5018 and 5169 Å (multiplet 42) reached the velocity  $-1400$  km/s. This is a typical velocity of an ejected shell in classical Fe II type novae. The half-width of the emission component was  $\sim 940$  km s $^{-1}$ . At the phase 2015b, the absorption component of the Fe II-line P Cyg profiles became stronger as well as in the Balmer lines, and the limiting velocities increased up to  $-4000$  km s $^{-1}$ . Such velocities of envelope ejection exceed velocities of fast high-luminosity Fe II type classical novae, but they are small for SNe. At that, the half-width of the emission component remained identical to that at the phase 2015a,  $940$  km s $^{-1}$ .

In June 13, 2015 spectrum in the SN phase, we observed a very wide emission extending to the blue side of the H $_{\beta}$  line to 18000 km/s with the maximum flux density at  $\lambda \sim 4640$  Å (it is marked as *emis.* in Fig. 4 below). The red part of this emission is overlaid by the absorption component of the H $_{\beta}$  line. Unfortunately, the emission is seen only in one spectrum, and we have no observations in the H $_{\alpha}$  line near the maximum brightness, so, it needs confirmation by independent observations. So far, the emission of so high-velocity outflow is the only available spectroscopic evidence that the event 2015b is a supernova. It is possible that in the spectrum of May 16, 2015 by [Duggan et al. \(2015\)](#) (6 days before maximum) a fragment of this emission was identified with He II 4686 Å. Besides, in description of that spectrum, there are no mentions about the strong Fe II lines,

which are seen in all our spectra. As a rule, the lines He II and Fe II are not observed in spectra simultaneously because of difference between ionization potentials at which these lines form, and, naturally, one can see either ones or the others depending on temperature of the excitation source.

In a case of a radially symmetric outflow of material at the velocity of  $18000 \text{ km s}^{-1}$ , the absorbing and emitting envelope components moving with the velocities less than  $4000 \text{ km s}^{-1}$  would be swept out by this material, or the high-velocity gas would underwent a fast deceleration. Nevertheless, a so unusual symbiosis of properties is observed in the spectrum. This symbiosis can be explained only by the axial asymmetry of outflow at the SN explosion. That is to say, the high-velocity gas was ejected along the polar axis whereas the slower outflow was occurring in equatorial directions. It is not excluded that in the equatorial plane there already was a dense gas disk which was formed at an earlier stage of evolution or at the phase 2015a and it prevented from distribution of high-velocity gas in the equatorial plane. For example, spectropolarimetry of SN 2009ip by [Mauerhan et al. \(2014\)](#) in the analogous phases 2012a and 2012b during its outburst in 2012 has shown that the outflows in these phases were strongly non-spherical, and the angles of polarization plane were orthogonal. In opinion by [Mauerhan et al. \(2014\)](#), in the case of 2009ip, the ejecta generated at the explosion of 2012a, in the phase 2012b were colliding in the equatorial plane with a flattened (toroidal) structure. Evidences of bipolar ejections at LBV explosions are not rare (this is seen in the Balmer line profiles, e.g., by [Barsukova et al. \(2014a\)](#), or in a bipolar structure of the "Homunculus" nebula around the galactic LBV-type star  $\eta$  Car). At the case of SN 2015bh, probably, there was a "shot" of high-velocity gas in the observer direction related with the phase 2015b, whereas an opposite ejection was overlapped by a body of a thick equatorial disk or a toroidal structure at a relatively small inclination angle between this structure and the line of sight.

The spectra of the object in the blue and green ranges obtained at the phase 2015b after it appeared from behind the Sun, i.e. at the secondary decay of brightness (176–374 days from the brightness maximum) are shown in Fig. 6, and the total spectrum in day 209 – in Fig. 5 (bottom). In blue spectra, strengthening of the short-wave emission component in  $H_\beta$  line profiles was seen, this component being located at the place of the absorption component early observed near the light maximum. The same emission components grew at the same part of Fe II profiles what led to appearance of an extended blend in the region  $\lambda 4400 - 4700 \text{ \AA}$  and  $5150 - 5450 \text{ \AA}$ . If there were no strong hydrogen lines, such a spectrum would be similar to that of SN Ic 1994I, 2003jd, 2010gx, 2004aw (see Fig. 4 by [Pastorello et al. \(2010\)](#)).

Changes in the  $H_\beta$  profiles are shown in Fig. 7. Note that the December 2015 spectrum was

obtained with the low spectral resolution. In June 13, 2015 spectrum, the absorption component extended to the short-wave side from  $-400$  to  $-4000$   $\text{km s}^{-1}$ . This velocity range in the profile was gradually filled with emission, and on March 10, 2016 we already see in the spectrum a strong emission with a peak at  $-1300$   $\text{km s}^{-1}$ . In the  $\text{H}_\alpha$  profiles shown in Fig. 8, the similar effect is seen (except a profile with the absorption component of June 13, 2015; at that time the red-range spectrum was not obtained). In the May 30, 2016 spectrum, the continuum was already lower than the noise level, but the  $\text{H}_\alpha$  profile remained emissive and kept the double shape.

The identical behavior was described at late stages of light curve of the luminous red nova NGC 4490-OT2011 (Smith et al. 2016). Some difference from the event 2015bh was a smaller range of the absorption component velocities, from 0 to  $-650$   $\text{km s}^{-1}$ , so, the blue emission wing of the  $\text{H}_\alpha$  profile was covered with the absorption only partly, and an emission hump was observed at  $-650$   $\text{km s}^{-1}$ . The maximum absorption depth in this profile, and then the maximum strength of emission were observed at the velocity of  $-280$   $\text{km s}^{-1}$ . These velocities are 4–5 times lower than those ones of SN 2015bh. Smith et al. (2016) give an entirely plausible explanation of such evolution of the profile: "a massive shell was ejected at these speeds and was initially seen in absorption, but as the underlying photosphere cooled (as indicated by the spectral evolution during the decline from peak) and as the optical depth dropped, the same dense shell is seen in  $\text{H}_\alpha$  emission. This likely indicates ongoing shock heating of this ejected shell". To explain transition from absorption to emission in 2015bh one should add a factor of fast expansion of the ejected shell ( $v_r$ , up to  $4000$   $\text{km s}^{-1}$ ) causing it to become optically thin quickly. Smith et al. (2016) interpreted the event NGC 4490-OT2011 as a luminous red nova, the merger in a massive system. As a rule, the expanding envelopes of luminous red novae do not transit to the optically thin phase at all, and if they do, it turns out to be cold ionized and even molecular gas, as in the case of V4332 Sgr. Note that the NGC 4490-OT2011 light curve had two maxima, and in the second outburst (with a cold-star spectrum) it achieved a record absolute magnitude  $-14^m$ . At merging of cores of massive stars, a shock wave forms, and when it comes out on the surface, the first brightness maximum is observed (an example is LRN 2015/M 101, also a massive system studied by Goranskij et al. (2016)).

#### 4 DISCUSSION OF RESULTS

The relation between SNe impostors and LBVs is established quite reliably. Some SNe IIn are also obviously related with LBVs. Specific evidences of these relations were considered in de-

tail by [Tartaglia et al. \(2016\)](#) and in studies cited there. However, only four impostors are known which eruptions led to appearance of SNe IIn. Besides the above-mentioned event 2009ip, these are 2010mc ([Smith, Mauerhan & Prieto 2014](#)), 2011ht ([Fraser et al. 2013](#)), and LSQ13zm ([Tartaglia et al. 2016](#)). SN 2015bh demonstrates a certain similarity with these objects, but there are differences both in light curves and in spectra. The nature of LBV explosions, which lead to "detonation" of more large-scale explosions of SNe still remains unclear, although there are several hypotheses explaining this phenomenon.

(1) PPI – "pulsation pair instability", related to massive formation of electron-positron pairs in cores of massive hot stars, which results in a reduction of radiation pressure, a partial collapse of a star and a thermonuclear explosion. The thermonuclear explosion stops the collapse and gives rise to ejection of the envelope. In this case, the repeated outburst can be explained by interaction between ejecta and dense circumstellar medium ([Woosley, Blinnikov & Heger 2007](#)). The detailed review of final stages of evolution and mechanisms of SNe in massive stars is given by [Heger \(2012\)](#). It was established that the thermal energy released at the collision of rapidly moving ejecta with the dense circumstellar medium may be higher than that of the core collapse. Note that the PPI mechanism is valid for stars with initial mass within  $80 - 280 M_{\odot}$ , and it can generate repeated eruptions of an impostor, similar to the case of SN 2009ip, and, eventually, leads either to the core collapse and formation of a black hole, or to a full destruction of the star (at the photodisintegration of nickel for a mass within the range  $130 - 280 M_{\odot}$ ).

(2) Core collapse of a faint supernova and interaction of ejecta with a medium ([Mauerhan et al. 2013](#)).

(3) Repeated outbursts related with approaching of components at elliptical orbits with the interaction in a binary system, and a final outburst at the merger or direct collision (this hypothesis was considered for SN 2009ip, in which several outbursts of an impostor were observed before the SN explosion ([Soker & Kashi 2013](#))).

(4) Last explosion of LBV (a SN impostor) followed by the core collapse (SN IIn) ([Tartaglia et al. 2016](#)).

These hypotheses were considered in detail by ([Tartaglia et al. 2016](#)). We think one more scenario is possible.

(5) Merger of components of a massive system with formation of a common envelope broken by the core collapse of one of stars being at a later evolutionary stage because of an excess of the critical mass (a failed luminous red nova in a massive binary system). In such a case, the process of the merger of stars does not need to end by merging of their cores, and then the SN explosion

leads to a binary system containing an optical remnant of a companion (the accretion donor) + a compact component.

The scenario determines if a SN is a final stage of evolution of a massive star finished by a compact object, or it is a single event in an LBV history. This question is to be solved by observations of remnants of similar double explosions. Some events were discovered as SN IIn (e.g., LSQ13zm), but then their relation with an impostor might be detected from archive data. Are all type IIn SNe related to previous LBV explosions? This question also requires special studies.

Now let us consider how each hypothesis agrees with observations of SN 2015bh.

(1) The PPI hypothesis. Can the spectral similarities of SN 2015bh with classical Fe II type novae we found in this outburst be interpreted in favor of this hypothesis? Classical novae can be attributed based on their spectra to one of two types, He/N and Fe II, or they can be "hybrid" with transition from Fe II to He/N at an outburst. [Williams \(2012\)](#) explains this difference by the origin of gas ejected in the explosion. The He/N type novae have in their spectra very wide emission lines (a high velocity of ejection) of elements higher ionization degree with the rectangular profiles and almost always without absorption components. This means that the gas is ejected at a thermonuclear runaway just from the white dwarf. Spectra of Fe II type novae at the initial decay of light curve are characterized by numerous Fe II lines of low ionization degree which were excited by atomic collisions, though in the far red range there are lines of CNO elements which are excited at recombination and fluorescence scattering. Profiles of these lines are rounded, more narrow and often have P Cyg-type absorption features of optically thick expanding gas. The intensities of the Fe II emissions decrease relatively slowly as the brightness decreases, and occasionally increase again in the episodes of "secondary maxima" which happen during several months after the beginning of the outburst. In the brightness maximum and in secondary maxima at the decay of brightness the emitting gas is colder than in other phases. At the early decay of brightness, Fe II novae display narrow absorptions of heavy elements of the iron peak. This means that the spectrum forms in the gas shell with the element composition close to the solar one. [Williams \(2012\)](#) assumes that this gas arises from the secondary component, a normal star rather than from a white dwarf. Probably, it is not even mixed with the explosion ejecta, and saturated with heavy elements generated in the process of evolution of the secondary star. Hydrodynamic calculations show that the radiation and the material thrown off the white dwarf stimulate the secondary component to lose the mass through the Lagrange points L1 and L3, and the shock from the orbital motion and accretion disk forms a circumstellar shell. At the same time, it was established that hybrid novae



develop only from the type Fe IIb novae (with broad lines in spectra), but not from Fe IIc ones (with narrow lines).

The arguments against the PPI hypothesis are as follows:

(a) The PPI hypothesis does not suppose that there is a component in a binary system. However, from the observed spectrum of SN 2015bh it follows that the composition of elements in the ejected shell and stellar wind at the outburst is close to solar one or only slightly evolved. As in the classical Fe II type novae, this material can originate in accretion from the secondary companion.

(b) Within the context of this hypothesis, the PPI event and thermonuclear explosion explain the phase 2015a, and the transformation of kinetic energy of ejecta into emission at interaction with circumstellar medium explains the 2015b phase. Photometric and spectral signs of SN at the 2015b phase noted by us previously, contradict the PPI hypothesis.

(c) The time of wave propagation inside the envelope released at the 2015a phase can be estimated as an interval between the end of the 2015a phase (the beginning of brightness decay at the moment JD 2457138, mag = 18<sup>m</sup>6 according to observations by Hoverton) and the outburst peak at the 2015b phase JD 2457165,  $V = 15^m35$ . This is equal to 27 days. Such a term is too large for propagation of dynamic changes, but it is typical for transfer of heat and radiation in massive envelopes (in the luminous red novae).

(2) Core collapse of a low-mass star, a faint supernova and interaction between the ejected shell and circumstellar medium. At that, the 2015a phase is interpreted as an SN IIP outburst, and the 2015b phase as interaction between the ejecta and environment. The examples of faint core-collapse SNe IIP reaching the absolute magnitude  $-14^m$  in the maximum brightness, 1999br and 2010id are adduced by [Tartaglia et al. \(2016\)](#). For SN 2015bh there are no evidences of a supernova outburst in the phase 2015a, although at the 2015b phase they are available: the rate of the secondary decay in the light curve is the same as the calculated  $^{56}\text{Co}$  decay rate, emission in the  $\text{H}_\beta$  line with the velocity up to 18000 km/s. These are arguments against the hypothesis about a faint SN.

(3) Approaching and final merging of components, a massive evolved star of mass 60-100  $M_\odot$  in a system with a star of mass 12–50  $M_\odot$  moving on an elliptic orbit. Paper by [Soker & Kashi \(2013\)](#) gives weighty arguments in favor of this hypothesis for SN 2009ip. We have no such arguments for the event 2015bh – repeated outbursts of the impostor or humps at the brightness decay at the burst of 2015b. Although [Thöne et al. \(2016\)](#) detected "short-term variability at least during 21 years" before the event of 2015. The merger of components even for massive stars leads to the phenomenon of a red nova, a cold explosion, but we have no spectral evidence of a red nova.

(4) The last explosion of LBV (the SN impostor) and a core collapse (SN II). The PPI event which provoked collapse of a massive core of LBV at a late stage of its evolution may be considered as the cause of explosion. The late stage of LBV evolution can be testified by unusually strong lines of iron. Iron could get to the star envelope due to the mixing. This is one of the promising hypotheses. In that case the explosion remnant will be a single black hole.

(5) Collapse of a core of a massive evolved LBV star in the system in a merger with a massive companion caused by exceeding critical mass of the core (a failed red nova in a massive binary system). E.g., in the galactic system  $\eta$  Car, in the orbit around LBV there is an O-class star of early or middle subclass with a mass within the range 30–60  $M_{\odot}$ , which passed a less evolutionary track than the main more massive component ([Corcoran & Ishibashi 2012](#)). Before the 2015b outburst, a gradual rise of the stellar brightness was observed which finished by a decline by  $1^m$ . The 2015a phase is usually called a SN impostor, but impostor light curves do not show gradual increase of brightness during outbursts. On the contrary, they show a decline typical for SNe (maybe, except SN 1954J). Such a brightness rise is typical for luminous red novae, and it is related with the formation of a common envelope at merger. The similar effect was observed in the luminous red novae V4332 Sgr, V1309 Sco, LRN 2015/M31 (M31N 2015-01a) and LRN 2015/M 101 (but it was absent in V838 Mon). The brightness decline by  $1^m$  before the luminous red nova outburst was observed in the case of V1309 Sco. [Barsukova et al. \(2014b\)](#) explain this decline by the merger of star cores and a slow shock from the star center which leads to transfer of the envelope in the expansion mode in the regime close to the adiabatic one. The term "slow shock" was first used by [Martini et al. \(1999\)](#) to explain the phenomenon of luminous red nova for V4332 Sgr.

At the merger of star cores in the massive red novae NGC 4490-OT2011 ([Smith et al. 2016](#)) and LRN 2015/M 101 ([Goranskij et al. 2016](#)), a shock wave formed, and, after it came out to the surface, the envelope passed to the mode of adiabatic expansion, which is accompanied by a deep weakening of brightness before the secondary maximum. Up to now, no spectra were obtained for the stage of common envelope formation in a luminous red nova, and, most probably, they are not similar to those of classical type Fe II novae. Such a spectrum of SN 2015bh at the 2015a phase can be explained by accretion of hydrogen-rich material from the companion onto the evolved star (LBV) at the phase of a common envelope formation, development of thermonuclear burning in a layer and release of additional energy by the accretion. At a high luminosity exceeding the Eddington limit, the mass outflow occurs with the typical rate for classical novae in outburst. At the merger of stars, the angular momentum is carried off with the material through the Lagrange point L1, which results in formation of a disk surrounding the system. Formation of a thick disk around

the massive star inside a common envelope can also be expected. In the moment when the critical mass was exceeded, the core collapse of evolved star occurred, and under such conditions, the explosion was asymmetric, with high-velocity gas outflow in the direction of axis of the inner disk. In the specific case of SN 2015bh, we observe the luminosity decline at the end of the 2015a phase, i.e. the slow shock already occurred, and the adiabatic expansion of envelope started. However, the core collapse stopped the adiabatic expansion of the envelope and interrupted the scenario of a luminous red nova. That is why the interrupted scenario can be called "a failed luminous red nova". Propagation of the shock wave inside the common envelope and its coming out to the surface can explain the light curve at the 2015b phase with its high luminosity and a sharp peak in maximum, along with a high temperature at the 2015b outburst decay (in contrast to luminous red novae), and transition of the envelope to the optically thin state. The abundance of hydrogen in the spectrum of 2015bh, the origin of which can be in the envelope of the less evolved companion, can argue for hypothesis (5). This hypothesis predicts a remnant being a binary system with a relativistic component, if the collapse occurred earlier than the total merger of the cores.

The latter hypothesis explains the events observed in the light curve and in the star spectrum in details. However, some components of the scenario (the high-velocity ejection in the  $H_\beta$  profile, the luminosity decline at the transition of the envelope to the mode of adiabatic expansion) are based on single observations and need a confirmation. The question of whether the already expanding envelope can transfer to the adiabatic mode due to a shock from within the star center remains open. The dynamical simulations are required. On April 7, 2015 Zhijiang Xu and Xing Gao observed a short burst which may be related with the exit of a primary, weaker shockwave. This observation should be verified. The question of whether the 2015bh event is a final episode in the evolution of a massive star is not yet solved, too. It will be answered by the study of the explosion remnant with large telescopes at a level of stellar magnitudes larger than 25<sup>m</sup>.

## 5 CONCLUSIONS

Spectra of the optical transient 2015bh/NGC 2770 in the phases of SN impostor and real SN obtained with BTA/SCORPIO are unusual, and they are similar to spectra of Williams Fe II type classical novae. From spectral data it was established that in the impostor phase (2015a), an optically thick expanding shell formed which was passed by a shock wave at the SN phase (2015b). Eventually, the shell was accelerated and transferred to the optically thin phase. Besides, we have revealed the absorption components in spectral line profiles related to the extended circumstellar

medium which partly accelerated by radiation pressure of SN explosion. Near brightness maximum, we have detected the emission component of high-speed,  $18000 \text{ km s}^{-1}$  ejecta in the  $H_{\beta}$  line profile along with slower moving, up to  $4000 \text{ km s}^{-1}$  absorption components, what suggests the asymmetric eruption. The light curve resembles the SN IIL ones with the rate of the secondary decline corresponding to the rates caused by the radioactive decay of  $^{56}\text{Co}$  isotope. In maximum, the SN reached the absolute magnitude  $M_V = -18^m14 \pm 0^m30$ .

The SN 2015bh progenitor is a luminous blue variable star (LBV) with the strong emission  $H\alpha$ , one of the brightest stars of the galaxy NGC 2770.

We consider that the most probable hypothesis to explain the SN 2015bh event is a core collapse of a more massive far-evolved star in a binary system breaking its merging with a less massive companion (a failed luminous red nova in a massive binary system). Arguments for and against other hypotheses were also considered. The core collapse of a single massive star induced by the PPI event is also possible.

## 6 ACKNOWLEDGMENTS

In the paper we used the Sloan Digital Sky Survey database, the NASA/IPAC Extragalactic Database (NED), the Hubble Space Telescope archive, the hosting site of images Flickr.com, the databases of supernovae by Rochester Astronomy and Sternberg Astronomical Institute of the Moscow University. The spectral and photometric observations performed in the Special Astrophysical Observatory of the Russian Academy of Sciences, their processing and analysis were financed by the Russian Science Foundation (RSF) by the Grant No.14–50–00043. The operation of the Russian 6 meter telescope BTA is financially supported by the Ministry of Education and Science of the Russian Federation. V.P.G., E.A.B. and A.F.V. thank the Russian Foundation for Basic Research (RFBR) for the financial support of this work with the Grant 14–02–00759. A.V.Zh. thanks RFBR for the support by the Grant 16–02–0758. The research by D.Yu.Ts. was partially supported by the RSF Grant 16–12–10519. The work by I.M.V. was partially supported by a Grant of the Slovak Information Agency SAIA.

## REFERENCES

- Afanasiev V. L., Moiseev A. V., 2005, *Astron. Lett.* **31**, 194  
 Anderson J. P., González-Gaitán S., Hamuy M., et al., 2014, *ApJ* **786**, 67  
 Barsukova E. A., Goranskij V. P., Valeev A. F., Kaisin S. S., 2014, *Variable Stars* **34**, No. 4, P. 1

- Barsukova E. A., Goranskij V. P., Valeev A. F., Zharova A. V., 2014, *Astrophysical Bulletin* **69**, 67
- Campana S., Thöne C. C., Leloudas G., et al., 2015, *Astronomer's Telegram* No. 7517
- Corcoran M. F., Ishibashi K., 2012, in *Eta Carinae and the Supernova Impostors*. Ed. K. Davidson & R. M. Humphreys (Springer), ApSS Library, **384**, P. 195
- de Ugarte Postigo A., Leloudas G., Thöne C. C., et al., 2015a, *Astronomer's Telegram* No. 7409
- de Ugarte Postigo A., Thöne C. C., Leloudas G., Aceituno F., 2015b, *Astronomer's Telegram* No. 7514
- Duggan G., Bellm E., Leloudas G., et al., 2015, *Astronomer's Telegram* No. 7515
- Elias-Rosa N., Benetti S., Tomasella T., et al., 2015, *Astronomer's Telegram* No. 7042
- Fraser M., Magee M., Kotak R., et al., 2013, *ApJ* **779**, L8
- Goranskij V. P., Barsukova E. A., Spiridonova O. I., et al., 2016, *Astrophysical Bulletin* **71**, 82
- Graham M. L., Sand D. J., Valenti S., et al., 2014, *ApJ* **787**, 163
- Heger A., 2012, in *Eta Carinae and the Supernovae Impostors*, Ed. K. Davidson & R. M. Humphreys (Springer), ApSS Library, **384**, P. 299
- Humphreys R. M., Davidson K., 1979, *ApJ* **232**, 409
- Humphreys R. M., Martin J. C., 2012, in *Eta Carinae and the Supernova Impostors*. Ed. K. Davidson & R. M. Humphreys (Springer), ApSS Library, **384**, P. 1
- Margutti R., Milisavljevic D., Soderberg A. M., et al., 2014, *ApJ* **780**, 21
- Martini P., Wagner R. M., Tomaney A. et al., *ApJ* **118**, 1034
- Mauerhan J. C., Smith N., Filippenko A. V., et al., 2013, *MNRAS* **430**, 1801
- Mauerhan J., Williams G. G., Smith N., et al., 2014, *MNRAS* **442**, 1166
- Modjaz M., Li W., Butler N., et al., 2009, *ApJ* **702**, 226
- Oke J. B., 1990, *AJ* **99**, 1621
- Pastorello A., Smartt S. J., Boticella M. T., et al., 2010, *ApJ* **724**, L16
- Pastorello A., Cappellaro E., Inserra C., et al., 2013, *ApJ* **767**, 1
- Richardson N., Artigau E., 2015, *Astronomer's Telegram* No. 7543
- Smith N., Mauerhan J. C., Prieto J. L., 2014, *MNRAS* **438**, 1191
- Smith N., Andrews J. E., van Dyk S. D., et al., 2016, *MNRAS* **458**, 950
- Soker N., & Kashi A., 2013, *ApJ* **764**, L6
- Tartaglia L., A. Pastorello A., Sullivan M., et al., 2016, *MNRAS* **459**, 1039
- Thöne C. C., Michalowski M. J., Leloudas G., et al., 2009, *ApJ* **698**, 1307
- Thöne C., de Ugarte Postigo A., Leloudas G., et al., 2016, in *Frontiers of Massive-Star Evolution and Core-Collapse Supernovae*. Symposium S16 at EWASS 2016. Paper No. 1133, abstract
- Van Dyk S. D., Schuyler D., Peng C. Y., et al., 2000, *PASP* **112**, 1532
- Vinko J., K. Sarneczky K., Vida K., 2015, *Astronomer's Telegram* No. 7541
- Williams R., 2012, *AJ* **144**, 98
- Woosley S. E., Blinnikov S., Heger A., 2007, *Nature* **450**, 390

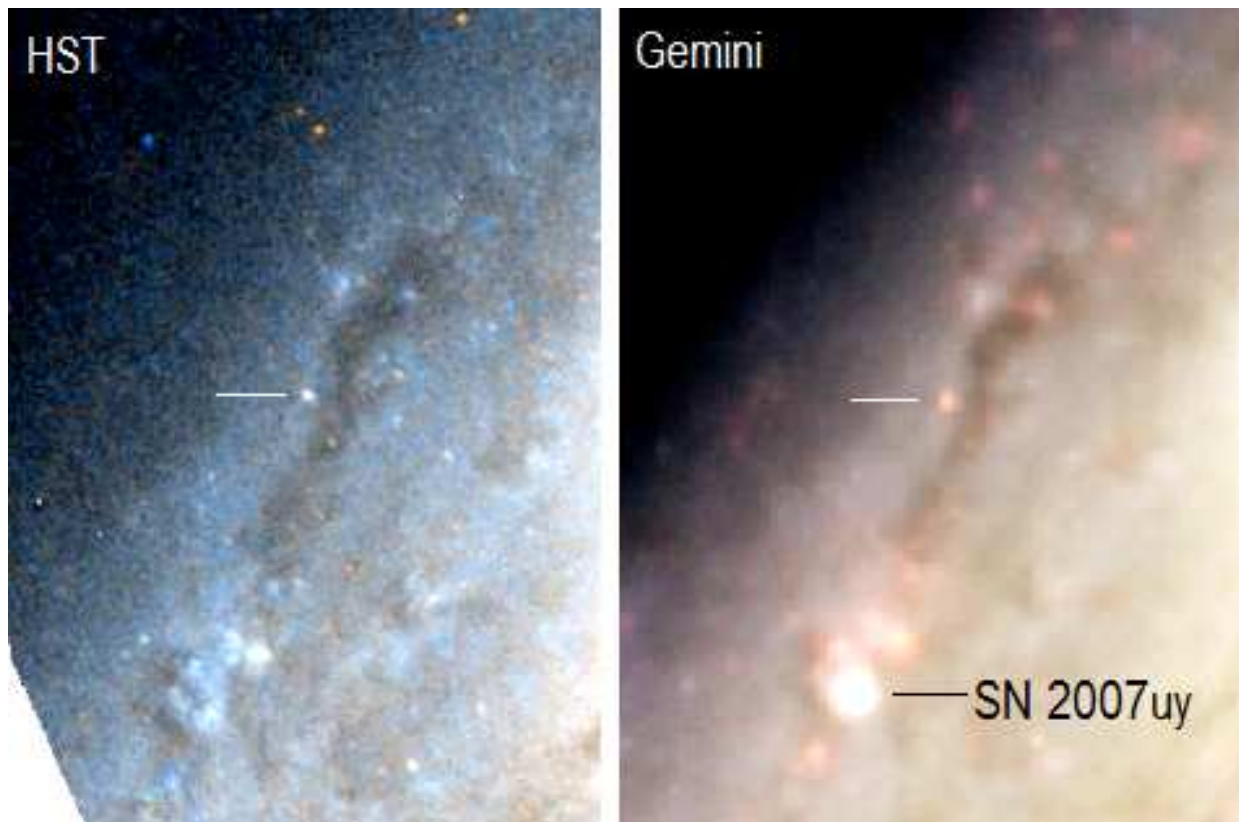


**Figure 1.** Fragments of high angular resolution images of the region  $40'' \times 60''$  around SN 2015bh the galaxy NGC 2770. Left: the image from the Space Hubble Telescope of December, 19, 2008; right: an image from the "Gemini" telescope of March 6, 2008. The progenitor is marked by the horizontal line.

This paper has been typeset from a  $\text{\TeX}/\text{\LaTeX}$  file prepared by the author.



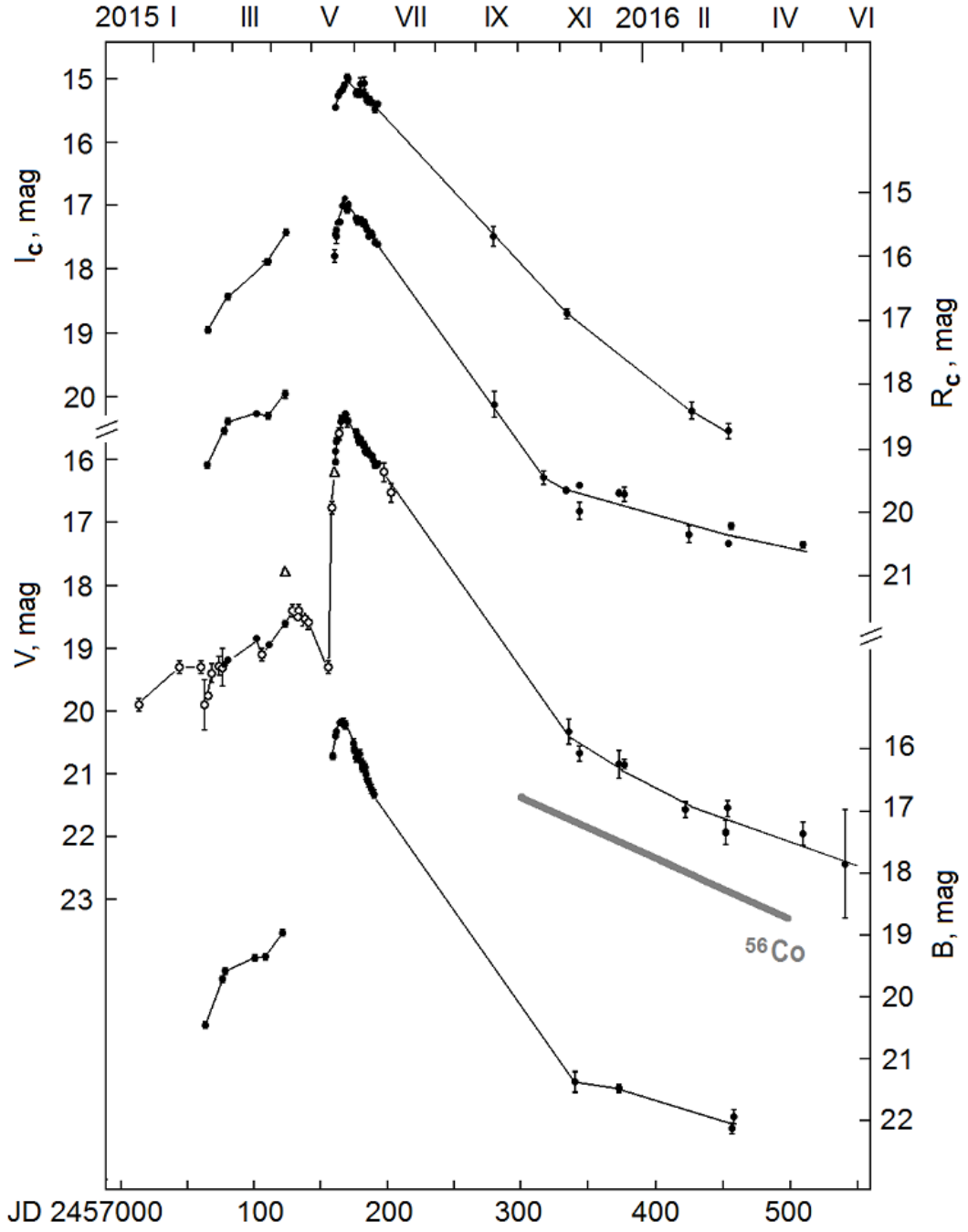


**Figure 2.** Light curves of SN 2015bh in 2015–2016 in  $B$ ,  $V$ ,  $R$ ,  $I$  bands (from bottom to top). The points are multicolor CCD observations including our ones and those ones cited in the text. The circles are observations from the collection by S. Hoverton obtained mainly with CCD without a filter. The triangles are observations by Zhijang Xu and Xing Gao. The gray line shows the average rate of brightness decay of SN I and II caused by radioactive decay of  $^{56}\text{Co}$ .

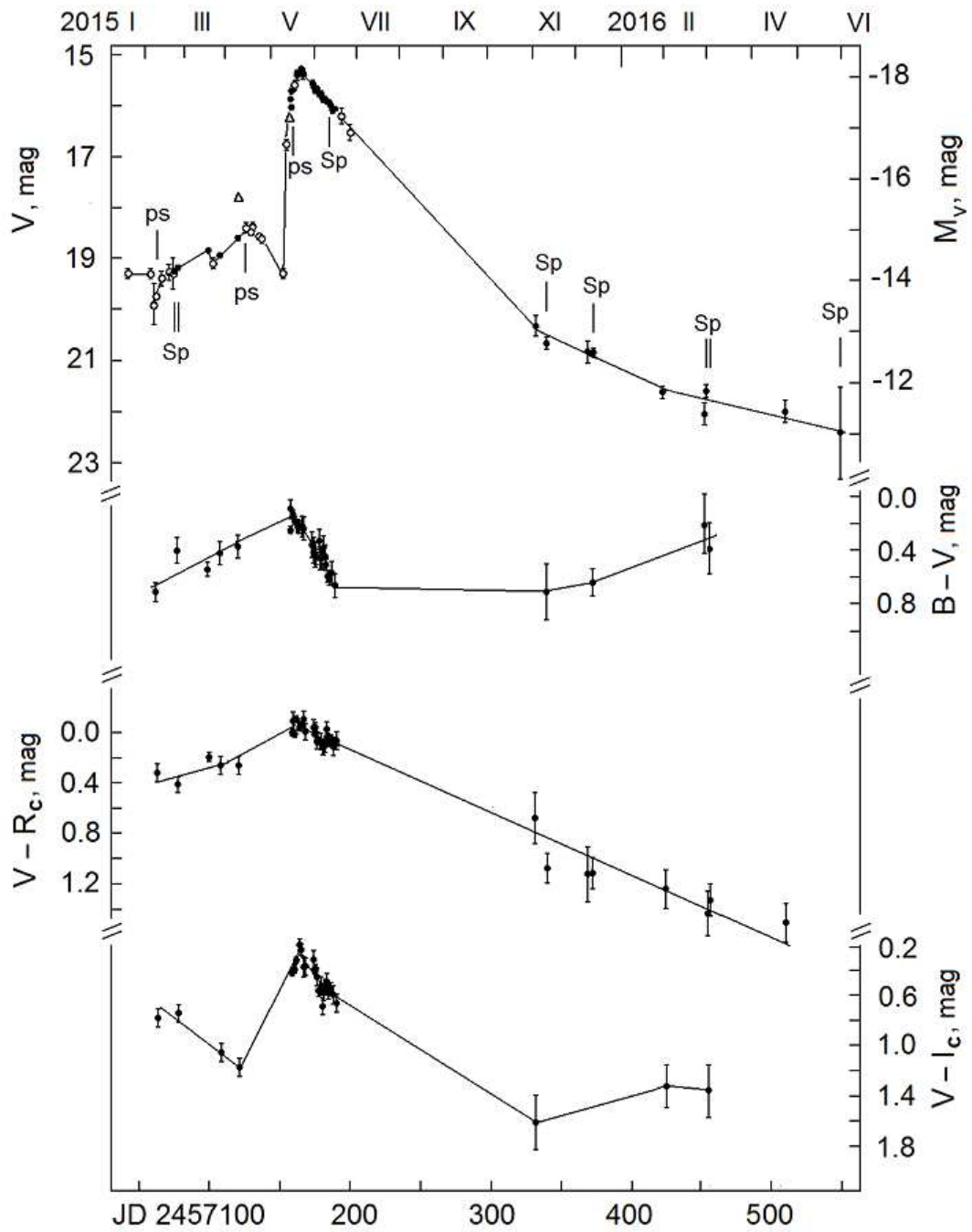


**Figure 3.** Light curve of SN 2015bh in the V band in the scale of absolute magnitudes and  $B - V$ ,  $V - R_C$  and  $V - I_C$  color index curves built from observations of 2015 – 2016. The moments of spectral observations taken in this search are marked by a label *Sp*, and other spectral observations published in Internet, or if their description are published, are marked by *ps*.

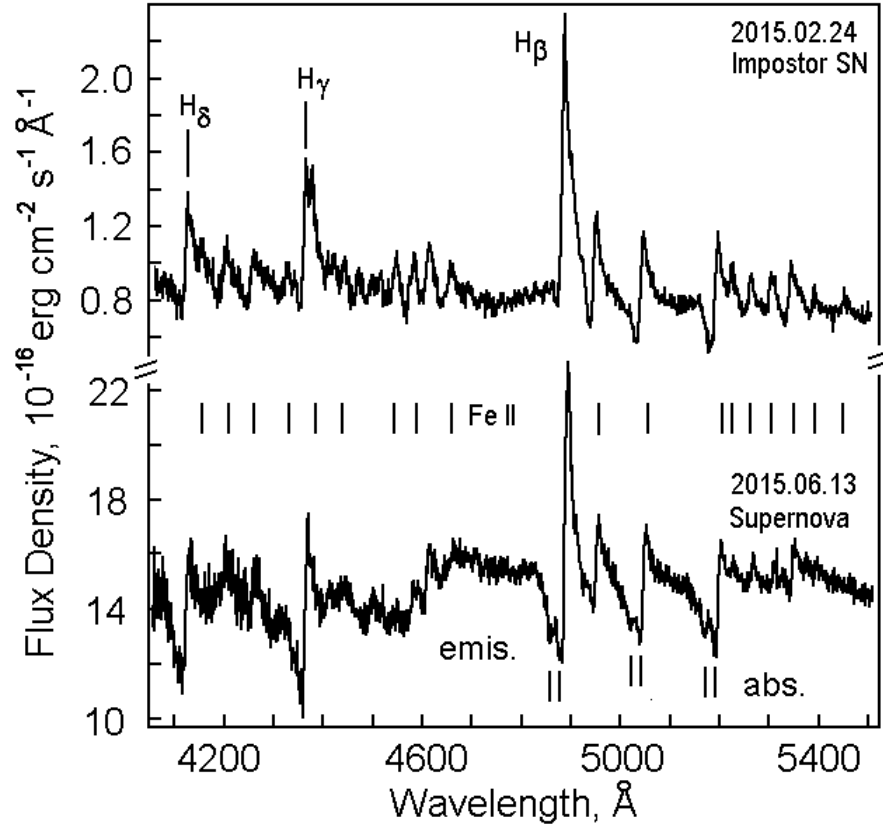


**Figure 4.** Spectra of SN 2015bh in the blue and green ranges at the impostor stage 2015a (top) and supernova stage 2015b in 22 days after the brightness maximum (bottom). *emis.* is a high-velocity emission component in the  $H_{\beta}$  line. The bottom spectrum shows double narrow components of the circumstellar medium (*abs.*) formed before 2015b.

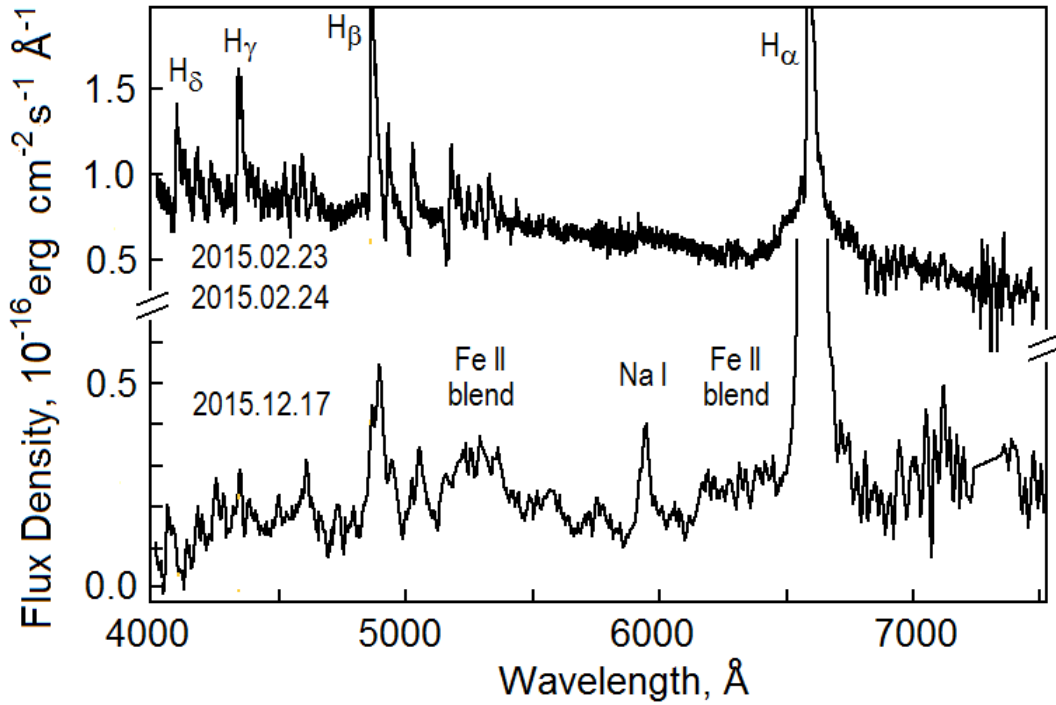


**Figure 5.** Full spectra of SN 2015bh at the phase 2015a and 2015b at the secondary brightness decay.

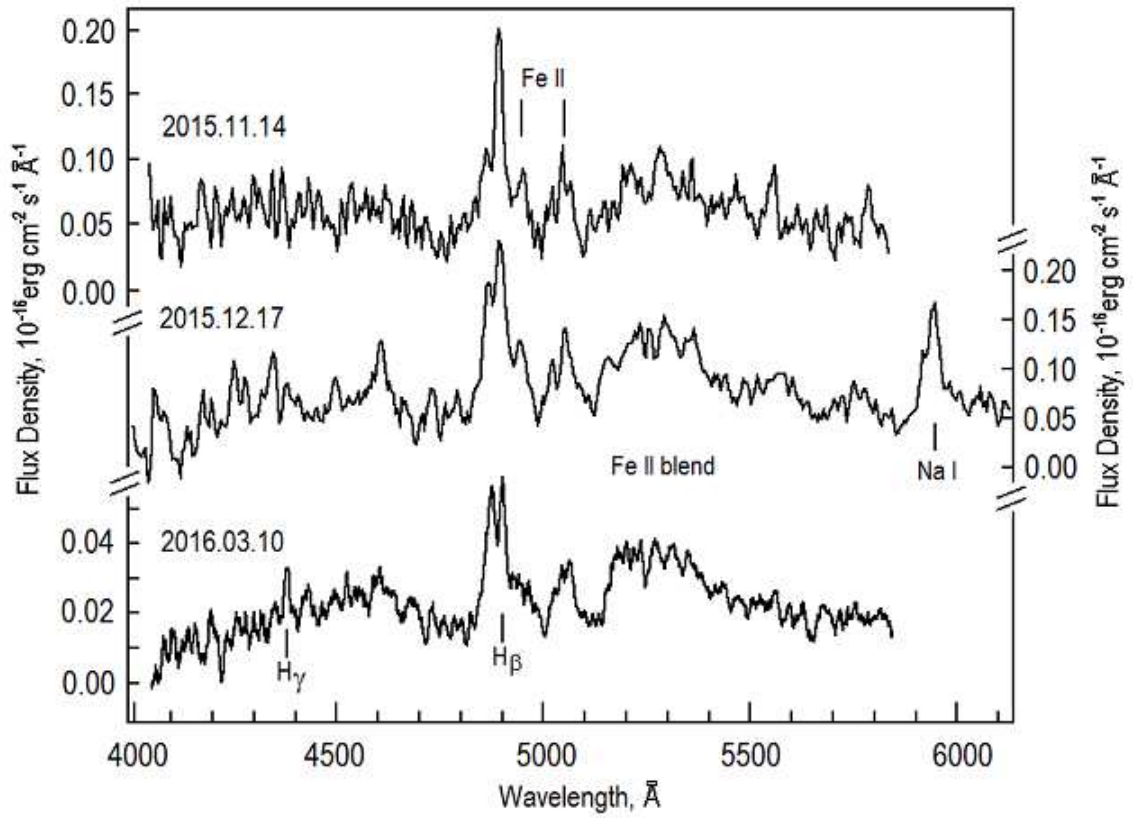


**Figure 6.** Spectral changes of SN 2015bh at the secondary brightness decay.

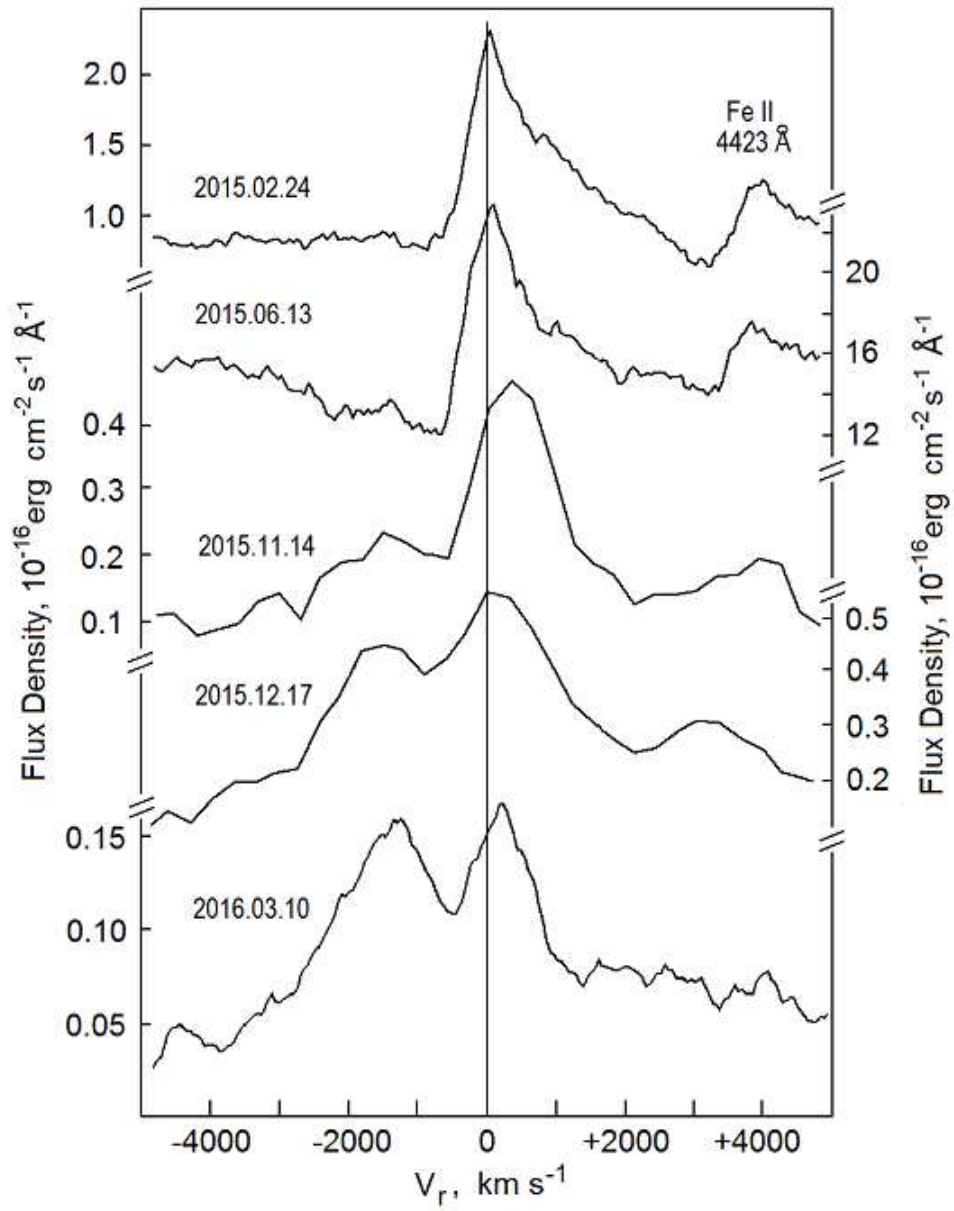


**Figure 7.** Profiles of the spectral line  $H\beta$  and their changes with time (from top to bottom).

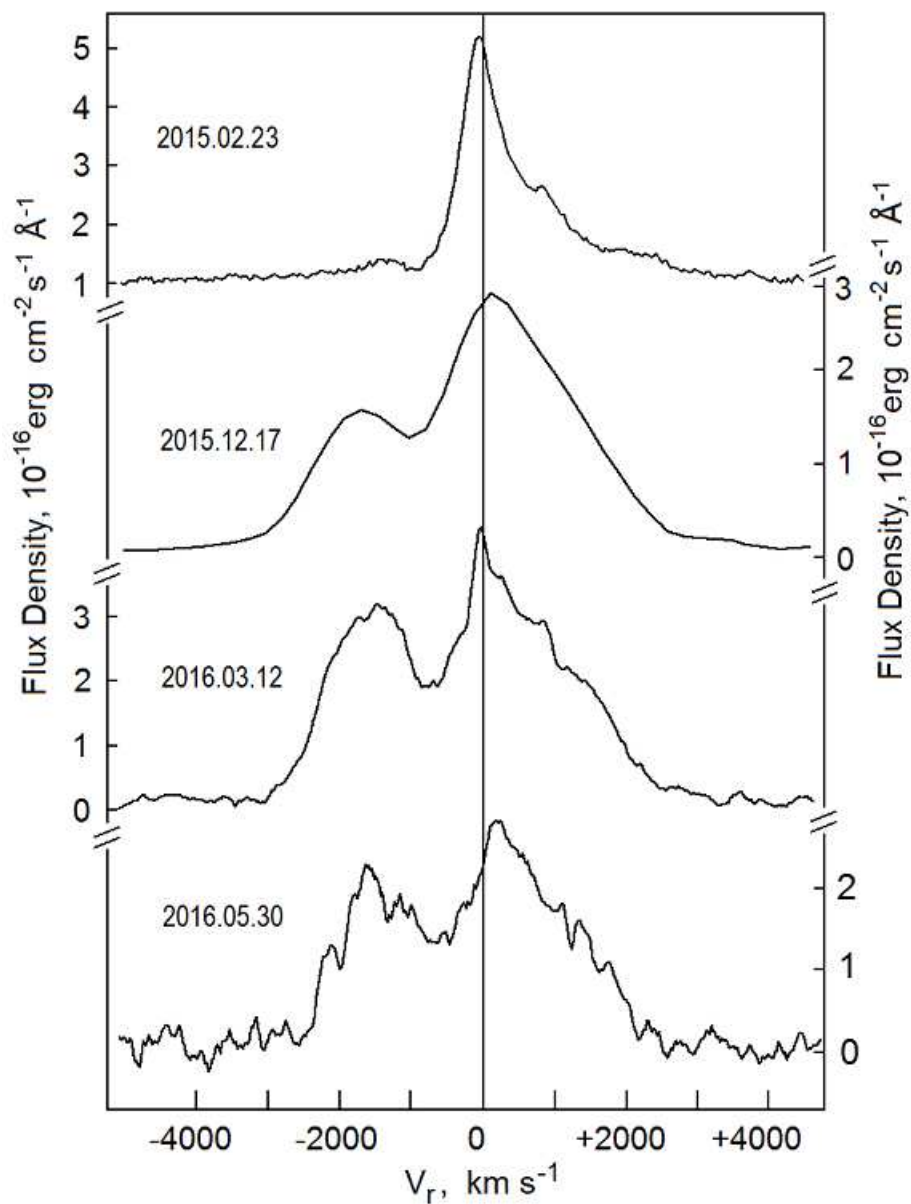


**Figure 8.** Profiles of the spectral line H $\alpha$  and their changes with time (from top to bottom).



Table 1. Photometry of SN 2015bh in NGC 2770

JD hel.24...	<i>B</i>	<i>V</i>	<i>R<sub>C</sub></i>	<i>I<sub>C</sub></i>	remark
57076.491	19.65 (5)	19.26 (5)	18.71 (4)	18.60 (5)	6m
57078.373	19.58 (8)	19.19 (5)	18.576 (40)	18.44 (5)	6m
57100.284	19.372 (50)	18.841 (30)	18.446 (20)	-	SO
57164.255	15.579 (40)	15.376 (20)	15.214 (20)	15.167 (40)	SO
57164.266	15.581 (40)	15.368 (20)	15.214 (20)	-	SO
57165.248	15.566 (40)	15.347 (20)	15.205 (20)	15.101 (40)	SO <sup>1)</sup>
57165.338	15.54 (5)	15.35 (3)	15.18 (4)	-	IW
57166.320	-	15.272 (20)	15.136 (20)	-	SO
57167.28	15.572 (60)	15.362 (50)	15.265 (40)	14.978 (50)	IW
57168.29	15.611 (70)	15.387 (50)	15.193 (50)	15.007 (50)	IW
57169.32	-	-	15.24 (6)	-	A2
57174.27	15.906 (70)	15.558 (50)	15.399 (50)	15.232 (50)	IV
57175.28	16.022 (80)	15.618 (20)	15.453 (50)	15.224 (50)	IV
57175.30	16.002 (70)	15.645 (20)	15.423 (50)	15.213 (50)	IV
57176.36	16.137 (70)	15.714 (50)	15.444 (50)	15.249 (50)	IV
57177.34	16.106 (50)	15.665 (30)	15.415 (50)	15.09 (1)	IV
57179.31	16.084 (70)	15.768 (50)	15.497 (50)	15.232 (50)	IV
57180.3	16.213 (60)	15.766 (50)	15.450 (40)	15.07 (1)	A5
57181.3	16.310 (60)	15.863 (50)	15.547 (50)	15.281 (50)	IV
57182.3	16.252 (60)	15.883 (50)	15.587 (40)	15.340 (40)	A5
57183.3	16.301 (60)	15.868 (50)	15.691 (40)	15.366 (40)	A5
57184.257	-	15.912 (20)	15.676 (40)	-	SO
57184.27	16.420 (70)	15.923 (20)	15.639 (30)	15.330 (40)	IV
57185.272	16.513 (30)	15.931 (20)	15.644 (20)	15.374 (40)	SO <sup>2)</sup>
57186.29	16.541 (70)	15.936 (20)	15.690 (40)	15.384 (40)	IV
57187.285	-	16.005 (30)	-	-	6m
57188.33	16.648 (70)	16.090 (50)	15.777 (40)	15.487 (50)	IV
57190.3	16.726 (60)	16.073 (50)	15.805 (50)	15.402 (40)	A5
57276.55	-	-	18.31 (20)	17.49 (15)	SO
57313.59	-	-	19.45 (11)	-	FL
57330.58	-	-	19.64 (10)	-	A5
57331.58	-	-	-	18.71 (8)	A5
57332.58	-	20.33 (20)	-	-	A5
57340.45	-	-	19.77 (14)	-	A5
57340.54	21.37 (17)	20.67 (12)	19.57 (2)	-	6m
57369.50	-	20.84 (22)	19.69 (3)	-	SO
57373.53	21.48 (6)	20.85 (08)	19.71 (11)	-	6m
57426.483	-	21.60 (12)	20.33 (2)	20.27 (20)	SO
57456.468	22.16 (9)	21.95 (18)	20.48 (3)	-	SO
57457.404	-	-	-	20.58 (11)	SO
57458.326	21.96 (12)	21.56 (12)	20.20 (5)	-	6m
57512.311	-	21.96 (17)	20.47 (5)	-	SO
57539.3	-	22.4 (9)	-	-	6m

**Remarks:**<sup>1</sup>  $U = 14.75$  (3)<sup>2</sup>  $U = 16.21$  (5)6m – the 6-m telescope BTA and the light reducer SCORPIO with the  $BVR_CI_C$  filters (Afanasiev & Moiseev 2005);

A2 – the 70-cm telescope AZT-2 of SAI in Moscow with the CCD Apogee Ap-7;

A5 – the 50-cm Maksutov meniscus telescope of the Crimean station of MSU with the CCD Apogee Alta U8300;

FL – the 60-cm Zeiss telescope of the Crimean station of MSU and  $UBVR_CI_C$ -photometer with the CCD camera FLI PL4022;

IV – the 1-m Zeiss telescope of Simeiz Observatory in Crimea with the CCD FLI PL09000;

IW – the 60-cm Zeiss telescope of Simeiz Observatory in Crimea with the CCD VersArray 512UV;

SO – the 1-m telescope of SAO RAS and the  $UBVR_CI_C$ -photometer with the CCD EEV 42-40.

**Table 2.** Spectra of SN 2015bh in NGC 2770 taken with BTA/SCORPIO

Date UT	JD hel.24...	$\Delta t$	$\epsilon$ , s	$\lambda$ , Å	R, Å	Grism	$\Delta v_r$ , km s <sup>-1</sup>	S/N
2015.02.23	57076.5160	-88	3600	5751 – 7501	5.5	VPHG1200R	-11.7	22
2015.02.24	57078.3933	-87	3600	4053 – 5847	5.0	VPHG1200G	-12.7	15
2015.06.13	57187.2982	+22	1800	4056 – 5850	5.0	VPHG1200G	-21.2	30
2015.11.14	57340.5885	+176	3600	4048 – 5846	5.0	VPHG1200G	+28.4	3
2015.12.17	57373.5602	+209	4800	3740 – 7877	14.6	VPHG550G	+20.5	2
2016.03.10	57458.2293	+293	3600	4043 – 5846	5.5	VPHG1200G	-18.3	2
2016.03.12	57460.3973	+295	2400	6024 – 7096	3.5	VPHG1800R	-19.4	4
2016.05.30	57539.3346	+374	2400	6025 – 7098	3.0	VPHG1800R	-24.9	<sup>1)</sup>

<sup>1</sup> Spectral continuum is lower than the noise level.